IJMF, Iranian Journal of Materials Forming, Vol. 4, No. 1, pp 52-62
Printed in The Islamic Republic of Iran, 2017

Prediction of Extrusion Pressure in Vortex Extrusion Using a Streamline Approach

M. Shahbaz*[1], J. G. Kim[2], R. Ebrahimi[3], H. S. Kim[2]

[1]Department of Materials Science and Engineering, School of Engineering, Urmia University, Urmia, Iran
[2]Department of Materials Science and Engineering, POSTECH, Pohang 790-784, Republic of Korea
[3]Department of Materials Science and Engineering, School of Engineering, Shiraz University, Shiraz, Iran

Abstract: Vortex extrusion (VE) is a severe plastic deformation technique which is based on the synergies between high strain accumulation and high hydrostatic pressure. Such a high amount of pressure places a mandate to seek the method for investigation of the load under processing conditions. For this, kinematically admissible velocity field and upper bound terms based on Bezier formulation are developed in order to investigate relative pressure in the VE process. Effects of reduction in area, relative length, twist angle, and friction factor in power dissipation terms are systematically analyzed. It is demonstrated that the increase in twist angle, area reduction and friction factor in the VE process increases the relative pressure, which the rates of these increase vary with twist angle. Moreover, the effect of the relative length is different in various frictional conditions. Results of conventional extrusion (CE) are in good agreement with those found by Avitzur for the effect of slug length and friction factor on the relative extrusion stress.

Keywords: Severe plastic deformation, Vortex extrusion, Bezier formulation, Upper bound theorem.

1. Introduction

Severe plastic deformation (SPD) is an efficient intense-straining method to produce bulk ultrafine grained (UFG)/nanostructured metallic materials [1-4]. Among various SPD techniques, processes that can impose a high amount of strain during one operation pass are more beneficial for productivity and microstructural evolutions.

In this regard, vortex extrusion (VE) [5-7] has been developed based on the synergies between high strain accumulation and high hydrostatic pressure, which are responsible for an effective grain refinement [8]. Such a high amount of pressure, which is more than the yield strength of materials, places a mandate to seek the method for investigation of the load under processing conditions and then of optimum die design for newly developed SPD processes. However, details of the VE process were not understood yet.

Recently, numerous research works have been performed to develop and analyze the torsion-based plastic deformation behaviors in SPD techniques, such as VE [5-7], twist extrusion (TE) [9, 10], and off-axis TE [11], by using numerical schemes, e.g. finite element method (FEM). In particular, the upper-bound theorem [12] has been used in order to predict processing loads for several SPD techniques, such as TE [13] and axisymmetric forward spiral extrusion [14]. Hoysan and Steif used a streamline-based method for analyzing steady state metal forming processes (e.g. extrusion and rolling) [15]. Materials with complicated, history-dependent, constitutive laws and a variety of metal/die interface conditions were considered in their analyses [15]. Chitkara and Celik analyzed the three-dimensional off-centric extrusion process of shaped sections from arbitrarily shaped billets through linearly converging and smooth curved dies using generalized CAD/CAM solutions [16]., In their study, a special velocity function was incorporated into the derived velocity fields to obtain a more realistic non-uniform metal flow and work hardening effect of the

Received by the editors November 1, 2016; Revised April 8, 2017 and Accepted April 15, 2017.
*Corresponding author (Mehrdads1@gmail.com)

material was considered [16]. Predictions of the deforming grid pattern, curvature of the extruded product as well as upper-bound to the extrusion pressures for a given reduction in area, material property, friction condition and off-centric positioning of the exit cross-section were considered as results of their study [16].

A generalized method based on the streamline approach was developed for the three-dimensional extrusion process of arbitrarily shaped sections through straightly converging dies [17]. In their study, for each case, a system of generalised kinematically admissible velocity fields are given to minimize the estimate of extrusion load [17]. Ponalagusamy *et al.* used a Bezier curve approach to design and develop the streamlined extrusion dies [18]. Narooei and Karimi Taheri developed a new three dimensional kinematically admissible velocity field using a Bezier formulation for the prediction of the strain field and extrusion pressure in the equal channel angular pressing (ECAP) processes of circular cross sections [19].

Beygelzimer et al. used the constructed kinematically admissible velocity field to qualitatively analysis of the metal flow mechanics in TE [20] and used a theoretical model of velocity field to investigate it experimentally [21].

In this study, relative pressure in the VE process was analyzed based on the Bezier formulation. The developed Bezier curve was used to obtain the kinematically admissible velocity field and then the power dissipation terms were calculated using the upper bound theorem. In particular, effects of reductions in area, relative length, twist angle, and friction factor on power dissipation terms and relative pressure were investigated.

2. Analysis method

VE die is schematically illustrated in Fig. 1. In VE die design (details are available elsewhere [5]), some dents are considered which force the materials to follow a vortex-like flow to form the die profile.

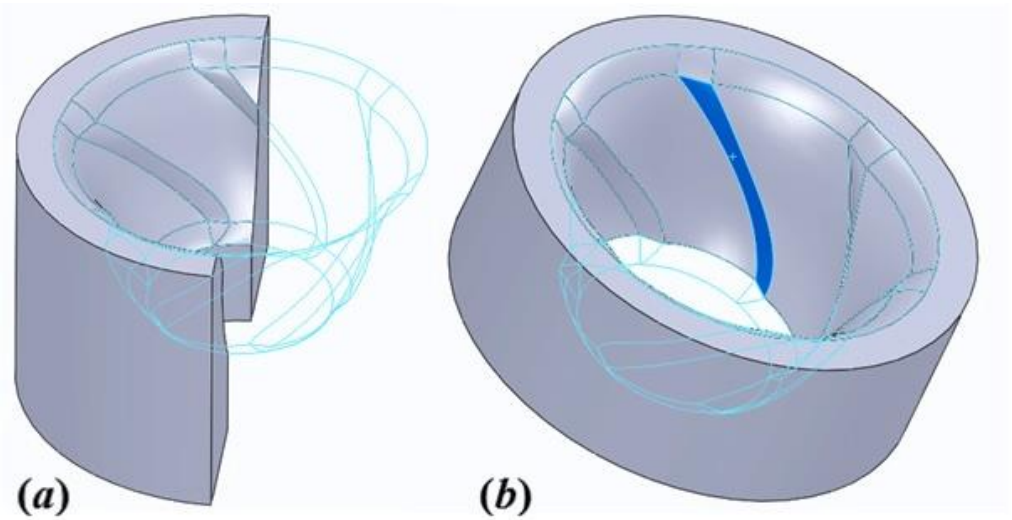

Fig. 1. Schematic illustration of (*a*) VE die design and (*b*) dent in main deformation zone of VE die.

In order to propose a general formulation for material flow in the VE die, cubic parametric Bezier curve with the control points of r_0, r_1, r_2, and r_3 is considered as follows [6]:

$$\vec{\gamma} = \overrightarrow{\gamma(t)} = \overrightarrow{r_0}(1-t)^3 + \overrightarrow{r_1}3t(1-t)^2 + \overrightarrow{r_2}3t^2(1-t) + \overrightarrow{r_3}t^3 \quad (1)$$

where $\vec{\gamma}$ is the vector equation of the streamline, and $\overrightarrow{r_0}$, $\overrightarrow{r_1}$, $\overrightarrow{r_2}$, and $\overrightarrow{r_3}$ are the position vectors of four control points.

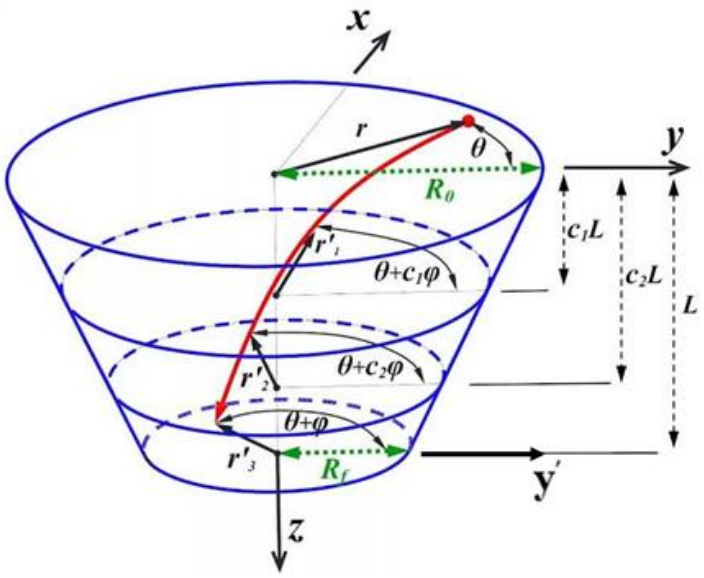

Fig. 2. Schematic of the material flow in the VE process.

As shown in Fig. 2, the position vector of point r_0 creates the radius r and angle θ with respect to the y axis in the entry circular section. The position vector of point r_3 creates the radius r_3' and angle $\theta + \varphi$ with respect to the y' axis in the exit circular section (Note: φ is the predetermined twist angle of the VE die). For the two remaining points of streamline, r_1 and r_2 at positions c_1L and c_2L inside the deformation zone, it is assumed that materials undergo a twist amount of $c_1\varphi$ and $c_2\varphi$, respectively (c_1 and c_2 are constants that vary between 0 and 1, and $c_2 > c_1$). Furthermore, it is assumed that the lateral surface of VE die forms a cone (Fig. 2).

Hence, the position vectors can be given as follows [6]:

$$\begin{aligned}
&\overrightarrow{r_0} = r\sin\theta\,\vec{\imath} + r\cos\theta\,\vec{\jmath}\\
&\overrightarrow{r_1} = r_1'\sin(\theta + c_1\varphi)\,\vec{\imath} + r_1'\cos(\theta + c_1\varphi)\,\vec{\jmath} + c_1L\vec{k}\\
&\overrightarrow{r_2} = r_2'\sin(\theta + c_2\varphi)\,\vec{\imath} + r_2'\cos(\theta + c_2\varphi)\,\vec{\jmath} + c_2L\vec{k}\\
&\overrightarrow{r_3} = r_3'\sin(\theta + \varphi)\,\vec{\imath} + r_3'\cos(\theta + \varphi)\,\vec{\jmath} + L\vec{k}
\end{aligned} \tag{2}$$

where $\vec{\imath}$, $\vec{\jmath}$, and $\vec{k}$ are unit vectors in the x, y, and z directions, respectively. Considering R_0 and R_f as the input and output radius of VE die, respectively, the values of r_1', r_2', and r_3' can be written as follows [6]:

$$r_i' = (1 - c_i)r + c_i\,{R_0 r}\big/{R_f} \tag{3}$$

In order to accommodate all points in the deformation zone, some parameters, such as u, q, and t, are introduced, which vary between 0 and 1 and follow from the following equation [6]:

$$\theta = q(2\pi),\ \ r = uR_0,\ z = tL \tag{4}$$

Equations (1)-(4) result the equation (5) [6]:

$$\overrightarrow{\gamma(t)} = f(u,q,t)\vec{\imath} + g(u,q,t)\vec{\jmath} + h(u,q,t)\vec{k} \tag{5}$$

where

$$\begin{aligned}
\mathrm{X} &= f(u,q,t) = uR_0(1-t)^3\sin 2\pi q + 3r_1't(1-t)^2\sin(2\pi q + c_1\varphi) + 3r_2't^2(1-t)\sin(2\pi q + c_2\varphi) + r_3't^3\sin(2\pi q + \varphi),\\
\mathrm{Y} &= g(u,q,t) = uR_0(1-t)^3\cos 2\pi q + 3r_1't(1-t)^2\cos(2\pi q + c_1\varphi) + 3r_2't^2(1-t)\cos(2\pi q + c_2\varphi) + r_3't^3\cos(2\pi q + \varphi),\\
\mathrm{Z} &= h(u,q,t) = 3t(1-t)^2c_1L + 3t^2(1-t)c_2L + t^3L
\end{aligned} \tag{6}$$

Using Eqs. (3)-(6), the positions of all points inside the deformation zone and the relationship between the coordinates $r, \theta,$ and z in the Cartesian coordinate system can be described.

In the following section, the kinematically admissible velocity field and then the upper bound terms will be developed using Eqs. (3)-(6).

2.1. Kinematically admissible velocity field and strain rate components

Considering that a velocity vector at any given point along a streamline is always tangent to it and the plastically deforming zone is bounded by the entry and exit planes, the velocity components for the incompressible materials in the *x*, *y*, and *z* directions can be expressed as follows [16]:

$$V_x = \frac{MX_t}{Z_t(X_uY_q - X_qY_u) + Z_q(X_tY_u - X_uY_t) + Z_u(X_qY_t - X_tY_q)}$$

$$V_y = \frac{MY_t}{Z_t(X_uY_q - X_qY_u) + Z_q(X_tY_u - X_uY_t) + Z_u(X_qY_t - X_tY_q)}$$

$$V_z = \frac{MZ_t}{Z_t(X_uY_q - X_qY_u) + Z_q(X_tY_u - X_uY_t) + Z_u(X_qY_t - X_tY_q)} \tag{7}$$

where M is a constant of integration and is obtained by considering the boundary condition ($V_z\big|_{t=0} = V_0$) as:

$$M = V_0\big|(X_uY_q - X_qY_u)\big|_{t=0} \tag{8}$$

where V_0 represents the ram velocity.

The general relation for strain rate components in terms of the velocity field, for Cartesian systems, can be written as [16]:

$$\dot{\varepsilon}_{ij} = \frac{1}{2}\left(\frac{\partial V_i}{\partial X_j} + \frac{\partial V_j}{\partial X_i}\right) \tag{9}$$

where,

$$\frac{\partial V_i}{\partial X_k} = \sum_{j=1}^{n}\left(\frac{\partial V_i}{\partial u_j}\frac{\partial u_j}{\partial X_k}\right) \tag{10}$$

2.2. Upper bound solution

The total power consumption J^* during the VE process through the die, sum of the internal power of deformation $(\dot{W}_{int})$, shear power ($\dot{W}_{S_t}$ at the entry and $\dot{W}_{S_e}$ at exit), and friction power $(\dot{W}_f)$, are computed via a kinematically admissible strain rate field that is derived from a kinematically admissible velocity field. Considering von-Mises materials, the terms related to J^* can be expressed as follows [16];

Internal power of deformation:

$$\dot{W}_{int} = \bar{\sigma}_m \int_V \sqrt{\frac{2}{3}\dot{\varepsilon}_{ij}\dot{\varepsilon}_{ij}}\, dV$$
$$= \frac{2\bar{\sigma}_m}{\sqrt{3}} \int_0^t \int_0^q \int_0^t \sqrt{\frac{1}{2}\left(\dot{\varepsilon}_{xx}{}^2 + \dot{\varepsilon}_{yy}{}^2 + \dot{\varepsilon}_{zz}{}^2\right) + \left(\dot{\varepsilon}_{xy}{}^2 + \dot{\varepsilon}_{xz}{}^2 + \dot{\varepsilon}_{yz}{}^2\right)}\, |detJ| \partial u \partial q \partial t \tag{11}$$

where $\bar{\sigma}_m$ represents the mean effective stress of the work hardening materials, which is replaced by the yield stress of the non-work hardening materials.

Power loss due to the velocity discontinuities in the material flow at entry:

$$\dot{W}_{S_i} = \frac{\bar{\sigma}_m}{\sqrt{3}} \int_0^q \int_0^u \sqrt{V_x^2 + V_y^2}\Big|_{t=0} |detJ|_{t=0} \partial u \partial q \tag{12}$$

Power loss due to the velocity discontinuities in the material flow at exit:

$$\dot{W}_{S_e} = \frac{\bar{\sigma}_m}{\sqrt{3}} \int_0^q \int_0^u \sqrt{V_x^2 + V_y^2}\Big|_{t=1} |detJ|_{t=1} \partial u \partial q \tag{13}$$

Power loss due to friction at the die-material interface:

$$\dot{W}_f = \frac{m\bar{\sigma}_m}{\sqrt{3}} \int_0^t \int_0^q \sqrt{V_x^2 + V_y^2 + V_z^2}\Big|_{u=1} sec\gamma_r \left|\frac{\partial(x,z)}{\partial(q,t)}\right|_{u=1} \partial q \partial t \tag{14}$$

The angle γ_r in Eq. (14) is the angle of inclination of the element of the die surface with respect to the projected surface of the element on the *XZ* plane [16]. Through considering Eqs. (11)-(14), the total power consumption can be obtained as follows:

$$J^* = \dot{W}_{int} + \dot{W}_{S_i} + \dot{W}_{S_e} + \dot{W}_f \tag{15}$$

Now, once the total power consumption, *J**, is obtained from Eq. (15), the upper limit to the average pressure, P_{avg} and relative pressure, P_{rel} for the vortex extrusion are given by;

$$P_{avg} = \frac{J^*}{A_0 V_0} \tag{16}$$

and

$$P_{rel} = \frac{P_{avg}}{\bar{\sigma}_m} \tag{17}$$

Proposed streamline is used as an input to mathematical modeling to obtain the kinematically admissible velocity field. The power dissipation terms and then the relative pressure are calculated for the processing parameters listed in Table 1. For all the analyses, $V_0 = 1\, mm/sec$ is assumed. All calculations were considered for the main deformation zone. The procedure used to solve integrals (11)-(14) is illustrated in Fig. 3.

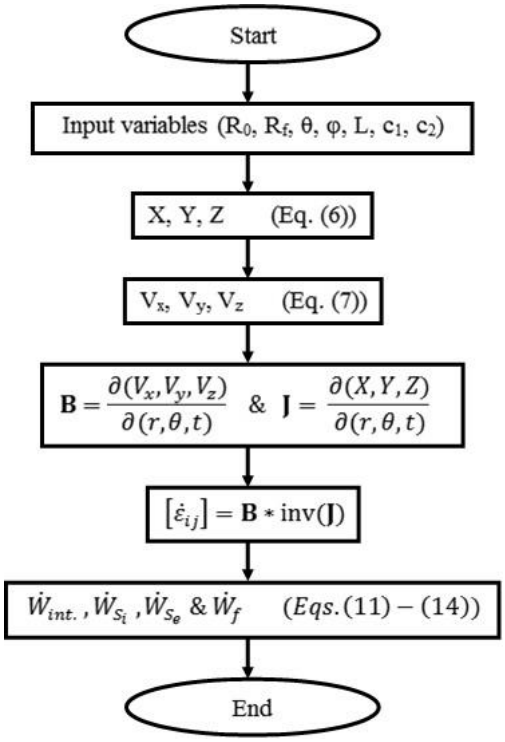

Fig. 3. Flowchart for solutions of integrals (11)-(14).

Table 1. Numerical parameters used in the mathematical modeling.

c_1	0.4
c_2	0.6
Reduction in Area (*RA*)	0, 0.1, 0.2, 0.3, 0.4, 0.5, 0.6, 0.7, 0.8, 0.9
Relative Length (RL=L/R_0)	0.84, 1, 1.263, 1.5
Constant Friction Factor (m)	0, 0.1, 0.25
Twist Angle (φ)	0 (CE), 30, 60, 90

3. Results and discussion

Figure 4 shows the components of the total power consumption (Eq. (15)) vs. twist angle and reduction in area (*RA*) for relative length ($RL=L/R_0$) of 0.84. In the proposed model, material paths for conventional extrusion ($\varphi = 0$) and VE ($\varphi \neq 0$) are for the conic and streamline, respectively. Increasing in the *RA*, in the constant *RL*, reduces the inclination of streamline in the predetermined twist angle. Therefore, based on Eq. (9), this will cause a decrease in all the right hand side terms of Eq. (15). These trends will be more perceptible for higher values of twist angle. On the other hand, with increasing in the *RA* (in constant *RL* and twist angle), the deformation, velocity discontinuity, and die-materials contact length will increase. Hence, the effect of the increased *RA* will be different for different values of φ, as follows;

- For $\varphi = 0$ (conventional extrusion); with increasing in the *RA*, all of the terms in the right hand side of Eq. (15) will increase as can be seen in Figs. 4*a*, *b*, and *c*.
- For $\varphi \neq 0$ (vortex extrusion); a decrease in streamline inclination due to an increase in *RA* will decrease the rate of increase in deformation power, which is more perceptible in higher values of twist angles, as can be seen in Fig. 4*a*. With increasing the twist angle, the decrease in the inclination of material path and hence decrease in power losses due to the velocity discontinuities in the material flow at entry and exit will dominate (Fig. 4*b*). Moreover, the decrease in inclination of material path will decrease the rate of the increase in power losses due to friction at the die-material interface (Fig. 4*c*).

Increasing the twist angle in the constant *RA* and *RL* will increase the deformation, velocity discontinuity, and die-material contact length, which will result in an increase in the internal power of deformation, shear power, and friction power (Fig. 4). The similar trend was seen for other *RL* listed in Table 1.

Figure 5 presents the components of total power consumptions (Eq. (15)) vs. twist angle and *RL* for *RA* = 0.6. In the constant *RA*, increasing in the *RL* will decrease the inclination of material path and so decrease the internal power (Fig. 5*a*). This decrease is more perceptible for higher values of twist angle. Figure 5*b* exhibits that the power losses due to a velocity discontinuity in the material flow at entry and exit are independent of *RL*. This is similar to the results reported in other research work [18]. Increasing in the *RL* will increase the die-material contact length, which will cause an increase in power loss due to friction in the die-material interface. However, the rate of this increase decreases with increasing in the twist angle. That is, for $\varphi \neq 0$, an increase in the *RL* will decrease the inclination of materials path and so decrease in friction power losses (Eqs. (7) and (14)). A similar trend was seen for other *RA* listed in Table 1.

Based on the obtained results for power terms and using Eq. (17), the effects of *RA*, twist angle, *RL*, and friction factor (m) on relative pressure are presented in Figs. 6 and 7. Figure 6 shows the relative pressure ($P_{rel.}$) vs. twist angle and *RA* for *RL* = 0.84 and different values of friction factor (*m*). Increasing in the *RA* increases the relative pressure; however, the rate of this increase will decrease with increasing the twist angle. Moreover, for constant values of *RA*, *RL*, and friction factor, increasing in the twist angle increases the relative pressure. Increasing in the friction factor (*m*) increases the relative pressure (Fig. 6*b*).

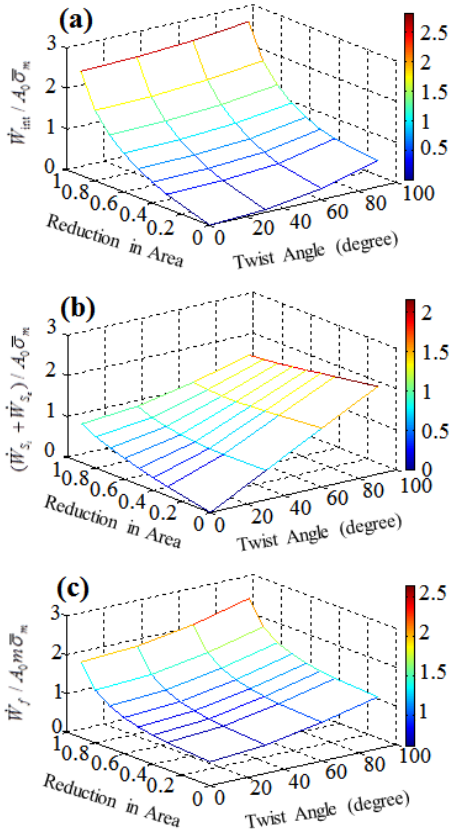

Fig. 4. Power losses due to (a) internal deformation, (b) velocity discontinuity surfaces at entry and exit, and (c) friction at the die-materials interface for *RL* = 0.84.

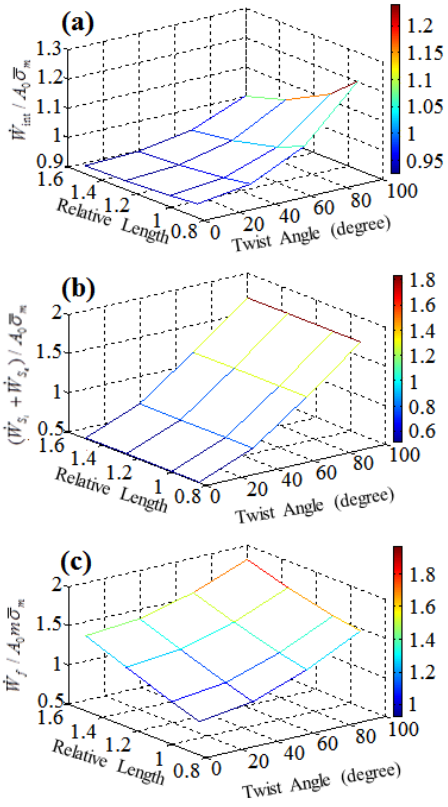

Fig. 5. Power losses due to (a) internal deformation, (b) velocity discontinuity surfaces at entry and exit, and (c) friction at the die-material interface for RA = 0.6 (R_0 = 9.5 mm).

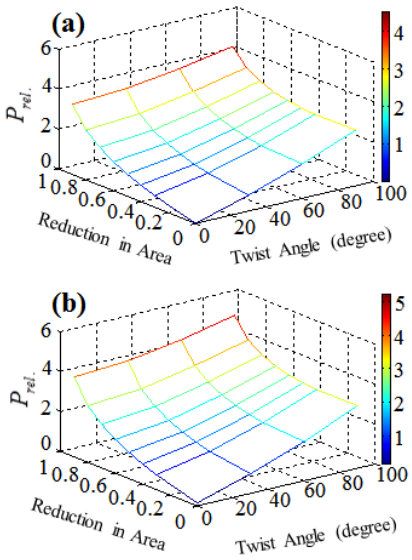

Fig. 6. Relative pressure ($P_{rel.}$) vs. twist angle and *RA* for *RL* = 0.84 and (a) *m* = 0, and (b) *m* = 0.25.

The effects of *RL* and twist angle on the relative pressure are represented in Fig. 7 for *RA* = 0.6 and different values of friction factor. For the frictionless condition (*m* = 0, Fig. 7*a*), the only term affected by the *RL* in the right hand side of Eq. (15) is the internal power. This would be affected by *RL*, which affects the relative pressure in a way that an increase in the *RL* will decrease the relative pressure. This is similar to the results represented in Fig. 5 that with an increase in the friction factor (Fig. 7*b*), the effect of power losses due to friction will dominate in conventional extrusion ($\varphi = 0$) and then the relative pressure will increase with an increase in the *RL*. In the case of conventional extrusion (CE), the obtained results from present study (Fig. 8) are in a good agreement with those found in a study done by Avitzur [12] in order to check the effect of slug length and friction factor on the relative extrusion stress. However, in vortex extrusion ($\varphi \neq 0$), the internal power will dominate on friction power in a way that with an increase in the *RL*, the relative pressure will decrease.

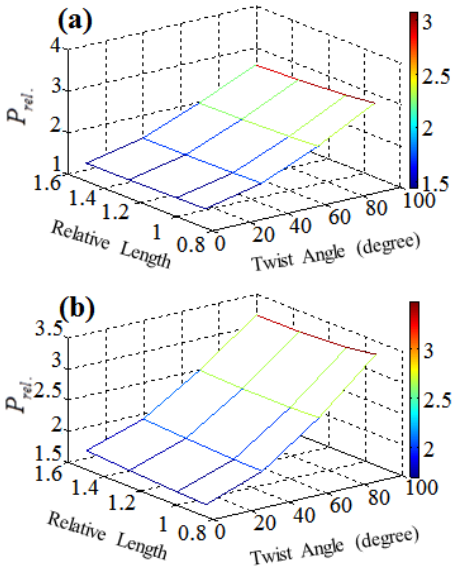

Fig. 7. Relative extrusion pressure ($P_{rel.}$) vs . twist angle and relative length for RA=0.6 (R_0=9.5mm) and (*a*) m=0, and (*b*) m=0.25.

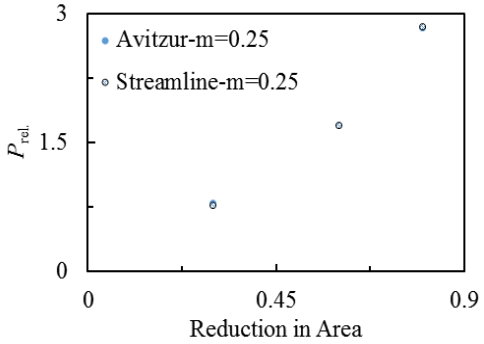

Fig. 8. Comparison of $P_{rel.}$obtained from Avitzur's analysis and streamline approach for CE with *RL*=0.84, m=0.25 and different values of the *RA*.

4. Conclusion

In the present study, the Bezier formulation was used to study the effect of reduction in area, relative length, twist angle, and friction factor on the load of the process in vortex extrusion. It was observed that with increasing the reduction in area, relative pressure increases. This trend in vortex extrusion occurs at a lower rate than in conventional extrusion. Friction factor increases the relative pressure for all the processing conditions. Increasing the twist angle increases the relative pressure. For frictionless condition, increasing the relative length decreases the relative pressure in all twist angles ($\varphi = 0$ and $\varphi \neq 0$) however, in frictional conditions ($m \neq 0$); for $\varphi = 0$ increasing the relative length increases the relative pressure and for $\varphi \neq 0$ relative pressure decreases with increasing the relative length.

Acknowledgements: The authors would like to thank Shiraz University, Iran and Pohang University of Science and Technology (POSTECH), South Korea for their financial support and research facilities used in this work. This work was supported by the research council office of Shiraz University through grant number 93-GR-ENG-15 and the National Research Foundation of Korea (NRF) grant funded by the Korea government (MSIP) (No. 2014R1A2A1A10051322).

5. References

[1] R.Z. Valiev and T.G. Langdon, Achieving exceptional grain refinement through severe plastic deformation: New approaches for improving the processing technology, *Metallic Materials Transection A*, 42 (2011) 2942-2951.

[2] A.Azushima, R. Kopp, A. Korhonen, D.Y. Yang, F. Micari, G.D. Lahoti, P. Groche, J. Yanagimoto, N. Tsuji, A. Rosochowski and A. Yanagida, Severe plastic deformation (SPD) processes for metals, *CIRP Annual Manufacturing and Technology*, 57 (2008) 716-735.

[3] Y. Estrin and A. Vinogradov, Extreme grain refinement by severe plastic deformation: a wealth of challenging science, *Acta Mateillia*, 61 (2013) 782-817.

[4] R.Z. Valiev, R.K. Islamgaliev and I.V. Alexandrov, Bulk nanostructured materials from severe plastic deformation, *Progress in Materials Science*, 45 (2000) 103-189.

[5] M. Shahbaz, N. Pardis, R. Ebrahimi and B. Talebanpour, A novel single pass severe plastic deformation technique: Vortex extrusion, *Materials Science and Engineering A*, 530 (2011) 469-472.

[6] M. Shahbaz, R. Ebrahimi, H.S. Kim, Streamline Approach to Die Design and Investigation of Material Flow in Vortex Extrusion Process, *Applied Mathematical Modelling*, 40 (2016) 3550–3560.

[7] M. Shahbaz, N. Pardis, J.G. Kim, R. Ebrahimi, H.S. Kim, Experimental and finite element analyses of plastic deformation behavior in vortex extrusion, *Materials Science and Engineering A*, 674 (2016) 472–479.

[8] Y. Beygelzimer, Grain refinement versus voids accumulation during severe plastic deformations of polycrystals: mathematical simulation, *Mechanics of Materials*, 37 (2005) 753-767.

[9] M.I. Latypov, I.V. Alexandrov, Y. Beygelzimer, S. Lee and H.S. Kim, Finite element analysis of plastic deformation in twist extrusion, *Computational Materials Science*, 60 (2012) 194-200.

[10] M.I. Latypov, M.G. Lee, Y. Beygelzimer, R. Kulagin and H.S. Kim, On the simple shear model of twist extrusion and its deviations, *Metals and Materials International*, 21 (2015) 569-579.

[11] Y. Beygelzimer, R. Kulagin, M.I. Latypov, V. Varyukhin and H.S. Kim, Off-axis twist extrusion for uniform processing of round bars, *Metals and Materials International*, 21 (2015) 734-740.

[12] B. Avitzur, Metal forming: processes and analysis, Original ed., McGraw-Hill Book Co., Reprint with revisions and corrections, New York (1979).

[13] M. Seyed Salehi, N. Anjabin and H.S. Kim, An upper bound solution for twist extrusion process, *Metals and Materials International*, 20 (2014) 825-834.

[14] S. Khoddam, A. Farhoumand and P.D. Hodgson, Upper-bound analysis of axi-symmetric forward spiral extrusion, *Mechanics of Materials*, 43 (2011) 684-692.

[15] S.F. Hoysan and P.S. Steif, A streamline-based method for analyzing steady state metal forming processes, *International Journal of Mechanical Science*, 34 (1992) 211-221.

[16] N.R. Chitkara and K.F. Celik, A generalised CAD/CAM solution to the three-dimensional off-centric extrusion of shaped sections: analysis, *International Journal of Mechanical Science*, 42 (2000) 273-294.

[17] N.R. Chitkara and K. Abrinia, A generalized upper-bound solution for three-dimensional extrusion of shaped sections using CAD/CAM bilinear surface dies, *Processing in 28th. International Matador Conference*, 18, April (1990).

[18] R. Ponalagusamy, R. Narayanasamy and P. Srinivasan, Design and development of streamlined extrusion dies a Bezier curve approach, *Journal of Materials and Processing Technology*, 161 (2005) 375-380.

[19] K. Narooei and A. Karimi Taheri, A new model for prediction the strain field and extrusion pressure in ECAE process of circular cross section, *Applied Mathematical Modelling*, 34 (2010) 1901-1917.

[20] Y. Beygelzimer, D. Orlov, V. Varyukhin, A new severe plastic deformation method: Twist Extrusion/Ultrafine Grained Materials II. *Proceedings of a symposium held during the 2002 TMS Annual Meeting I Seattle*, Washington, February 17-21, 2002/ Ed. by Y.T. Zhu, T.G. Langdon, R.S. Mishra, S.L. Semiatin, M.J. Saran, T.C. Lowe, TMS, (2002) 297-304.

[21] Y. Beygelzimer, A. Reshetov, S. Synkov, O. Prokof'eva, R. Kulagin, Kinematics of metal flow during twist extrusion investigated with a new experimental method. *Journal of Materials Processing and Technology*, 209 (2009) 3650-3656.

پیش بینی نیروی اکستروژن گردابی با استفاده از خطوط جریان

مهرداد شهباز[1]، جونگی کیم[2]، رامین ابراهیمی[3]، هیونگ سئوپ کیم[2]

[1] بخش مهندسی مواد، دانشکده فنی، دانشگاه ارومیه، ارومیه، ایران
[2] بخش مهندسی مواد، دانشگاه علم و تکنولوژی پوهانگ، پوهانگ، کره جنوبی
[3] بخش مهندسی مواد، دانشکده مهندسی، دانشگاه شیراز، شیراز، ایران

چکیده: اکستروژن گردابی بعنوان یک روش تغییر شکل پلاستیک شدید دسته بندی می‌گردد که بر پایه‌ی اثر همزمان اعمال کرنشهای پلاستیک شدید و مقادیر بالای فشار هیدروستاتیک است. اعمال چنین مقادیر بالای فشار لازمه تعیین روشی برای تحقیق و پیش بینی نیروی فرآیند تحت شرایط مطرح در روش است. برای این منظور، در تحقیق حاضر با بهره‌گیری از تئوری کران بالایی بر پایه میدان سرعت قابل قبول بدست آمده از فرمولاسیون بزییر، فشار نسبی مطرح در فرآیند اکستروژن گردابی بررسی و پیش بینی شد. تاثیر کاهش سطح مقطع، طول نسبی، زاویه پیچش و فاکتور ثابت اصطکاک بر ترم‌های اتلاف انرژی مطرح در تئوری کران بالایی بررسی گردید. نشان داده شد که با افزایش زاویه پیچش، کاهش سطح مقطع و فاکتور ثابت اصطکاک، فشار نسبی افزایش می‌یابد بگونه ای که نرخ این افزایش تحت تاثیر زاویه پیچش است. همچنین نشان داده شد که تاثیر طول نسبی بر فشار نسبی فرآیند در شرایط مختلف اصطکاکی متفاوت است. نتایج بدست آمده برای اکستروژن ساده همخوانی خوبی با نتایج تحقیق انجام شده توسط اویتزر در بررسی اثر طول نسبی و فاکتور ثابت اصطکاکی بر فشار نسبی اکستروژن ساده، دارند.

کلمات کلیدی: تغییر شکل پلاستیک شدید، اکستروژن گردابی، فرمولاسیون بزییر، تئوری کران بالایی.